International Journal of Biological Macromolecules 204 (2022) 9–18

Contents lists available at ScienceDirect

International Journal of Biological Macromolecules

journal homepage: www.elsevier.com/locate/ijbiomac

Osmundea sp. macroalgal polysaccharide-based nanoparticles produced by flash nanocomplexation technique

Sónia P. Miguel [a,b,*], Jorge Loureiro [a], Maximiano P. Ribeiro [a,b], Paula Coutinho [a,b,*]

[a] CPIRN-UDI/IPG, Centro de Potencial e Inovação em Recursos Naturais, Unidade de Investigação para o Desenvolvimento do Interior do Instituto Politécnico da Guarda, Avenida Dr. Francisco de Sá Carneiro, No. 50, 6300-559 Guarda, Portugal
[b] CICS-UBI, Centro de Investigação em Ciências da Saúde, Universidade da Beira Interior, Avenida Infante D. Henrique, 6200-506 Covilhã, Portugal

ARTICLE INFO

Keywords:
Macroalgal polysaccharide
Flash nanocomplexation
Nanoparticles

ABSTRACT

The macroalgae-derived polysaccharides' biological potential has been explored due to their attractive intrinsic properties such as biocompatibility, biodegradability, and their ability to conjugate with other compounds. In particular, in the drug delivery systems field, the anionic macroalgae polysaccharides have been combined with cationic compounds through ionotropic gelation and/or bulk mixing. However, these techniques did not assure reproducibility, and the stability of nanoparticles is undesired. To overcome these limitations, herein, the polysaccharide extracted from *Osmundea* sp. was used to produce nanoparticles through the flash nanocomplexation technique. This approach rapidly mixed the negative charge of macroalgae polysaccharide with a positive chitosan charge on a millisecond timescale. Further, diclofenac (an anti-inflammatory drug) was also incorporated into complex nanoparticles.

Overall, the gathered data showed that hydrodynamic diameter nanoparticles values lower than 100 nm, presenting a narrow size distribution and stability. Also, the diclofenac exhibited a targeted and sustained release profile in simulating inflammatory conditions. Likewise, the nanoparticles showed excellent biological properties, evidencing their suitability to be used to treat inflammatory skin diseases.

1. Introduction

The use of marine recourses in the biomedical field has been gaining relevant attention in the last few years. Indeed, several reports have already demonstrated the beneficial effects of marine organisms on human health.

Among the different bioactive compounds (polysaccharides, polyunsaturated fatty acids, and phlorotannins) obtained from macroalgae, considerable effort has been made to evaluate the potential of polysaccharides (PS) on functional foods, cosmeceuticals, and pharmaceuticals.

The macroalgae PS possess advantages like their excellent biocompatibility, charge properties, and high abundance. Also, it was proved that the PS has essential properties such as anticoagulant, antithrombotic, immunomodulatory ability, antitumor, antioxidant and anti-inflammatory activity, making them promising bioactive products with a wide range of applications, since from wound management, regenerative medicine, biosensors to development of drug delivery systems [1].

The potential of macroalgae PS has been studied in drug delivery systems applications since they possess hydrophilic surface groups like hydroxyl, carboxyl and sulphate groups, which interact easily with biological tissues. Further, another potential of the algae-derived PS is their anionic character which avoids aggregation during blood circulation since the interaction with serum proteins is reduced [2,3].

In this way, the PS has been used to produce the nanoparticles (NPs) using methods like solvent evaporation, nanoprecipitation, emulsification, and ionic gelation. Moreover, the potential of the protein-PS complexation as drug delivery systems has been recently outlined in a recent review [4,5]. In general, all methods require the use of organic solvents to form the NPs, which are hazardous to the environment and the physiological system. Besides, the methods are commonly laborious with multiple preparation steps, which can cause severe batch-to-batch variations, impairing the clinical translation. Moreover, the mixing of polyelectrolytes is typically achieved through manual mixing, vortex, or drop-wise addition, revealing poor reproducibility and quality of NPs

* Corresponding authors at: CPIRN-UDI/IPG, Centro de Potencial e Inovação em Recursos Naturais, Unidade de Investigação para o Desenvolvimento do Interior do Instituto Politécnico da Guarda, Portugal.
E-mail addresses: spmiguel@ipg.pt (S.P. Miguel), coutinho@ipg.pt (P. Coutinho).

https://doi.org/10.1016/j.ijbiomac.2022.01.180
Received 16 November 2021; Received in revised form 26 January 2022; Accepted 28 January 2022
Available online 2 February 2022

[6–10].

Thus, the flash nanocomplexation technique arises as a continuous and reproducible method to produce NPs through the ionic interactions, propelling the scale-up production of NPs for clinical translation. Through this strategy, a rapid mixing between the opposite compounds on a millisecond timescale is promoted. The electrostatic interactions between oppositely charged polymer units cause complexation in the controlled impingement jet mixer, leading to the fabrication of uniform nano-complexes with the desired shape, size and surface charge [1,11,12]. Moreover, this highly reproducible technique consumes low energy and requires a short processing time.

In addition, the introduction of polyelectrolyte solution in a small mixing chamber generates a suspension of polyelectrolyte NPs stabilised on the particle surface, offering control over size, narrow size distribution and higher encapsulation efficiency and loading level for therapeutic payloads.

This evidence was already verified by Zhiyu He et al., who used the flash nanocomplexation technique to produce scalable core-shell structured nanoparticles of L-Penetratin/insulin nanoparticles coated with hyaluronic acid. This method enabled the control in the size of NPs, generating core-shell structure with a high encapsulation efficiency of insulin (97%) and payload capacity (67%) [10].

In turn, Ke et al. produced curcumin-loaded NPs by bulk mixing and flash nanocomplexation techniques. The authors verified that the bulking mixing process leads to the precipitation of some compounds, indicating low mixing efficiency. In contrast, the flash nanocomplexation method promoted the production of NPs with the same particle size and size distribution, which were generated during 1 h, highlighting their potential for translation to industrial production [13].

So, in this work, the Osmundea sp.- PS was combined with CS to produce NPs using the flash nanocomplexation technique, favouring the electrostatic interactions between the negatively charged sulphate groups of PS and positively charged amine groups of CS. To the best of our knowledge, the use of polysaccharides from *Osmundea* sp. in the drug delivery system production has not yet been reported. The *Osmundea* sp. (Rhodophyta) is a red macroalgae characterised by a high content of sulphate groups, protein and sugars, which are relevant for biomedical applications [14,15]. The structure, classification and extraction methodologies of algal polysaccharides related issues have been discussed extensively in several reviews [16,17]. In addition, the macroalgae polysaccharides, namely the sulphated polysaccharides, exhibit promising properties to be used in wound regeneration since it is noteworthy that these polysaccharides improved the proliferation of the fibroblasts, promoting wound closure while hindering scar formation. Besides, several commercial skincare products are based on the properties of these polysaccharides, like Extract Codiavelane®, Gelcarin® PC 379, Chlorofiltrat® Ulva HG, among others [18,19]. The specific chemical characterisation of the *Osmundea* sp.-polysaccharide from the Galicia coast and extracted from the autoclave process has not yet been performed. Due to this reason, in this work, the chemical properties of extracted *Osmundea* sp.- polysaccharide was characterised.

Apart from this, the development of algae polysaccharides-chitosan based nanoparticles has been reported in the literature, demonstrating the excellent suitability of these nanocarriers for different biomedical applications. Huan et al. produced and characterised the fucoidan-chitosan nanoparticles incorporating curcumin for oral delivery system and verified that the nanoparticles were effective pH-sensitive carriers [20]. In turn, Grenha et al. developed chitosan-carrageenan for the drug delivery system [21]. As main findings, the authors observed that the nanoparticles showed biocompatibility, demonstrating high potential for biomedical applications such as drug delivery and tissue engineering. Further, Thai et al. selected chitosan and alginate to load lovastatin, where in vivo results revealed that the nanoparticles are safe, nontoxic and might be applied to lower serum cholesterol in animal models as well as humans [22].

On the other hand, the use of chitosan-based nanoparticles for skin treatment is a topic widely reported and validated [23–25]. Indeed, the biological properties of chitosan, like the hemostatic effect, the ability to inhibit microbial growth and accelerate wound healing, have been widely described and outlined as very attractive and effective in wound management applications [26–28].

Herein, an anti-inflammatory drug (Diclofenac (DLF)) was selected as a model drug to incorporate into nanoparticles aims to obtain a drug delivery system able to control the inflammation process in inflammatory skin diseases. After producing the nanosystems, their morphological, physical and biological properties were characterised.

Thus, the main goal of this pioneering work was to demonstrate the suitability of flash nanoprecipitation as an innovative production method (reproducible, rapid, without the use of organic samples, ready-to-use) of biocompatible nanocarriers with the potential to be used in the control of inflammatory skin disorders.

2. Material and methods

2.1. Materials

Osmundea sp. macroalgae samples were directly recovered from the Galicia coats by the partners from the University of Vigo.

Dimethyl sulfoxide (DMSO) was purchased from Appli Chem. Panreac (Barcelona, Spain). Sodium hydroxide ($NaHCO_3$) and Ethanol were acquired from José Manuel Gomes dos Santos (Odivelas, Portugal); Chitosan (CS) (LMW, 50–190 kDa), Diclofenac sodium salt (DLF), Dulbecco's modified Eagle's medium (DMEM)-F12, ethylenediaminetetraacetic acid (EDTA), fetal bovine serum (FBS), phosphate-buffered saline (PBS), trypsin were purchased from Sigma-Aldrich (Sintra, Portugal). Normal human dermal fibroblasts (NHDF) and Human epidermal keratinocytes (HEK) cells were acquired from PromoCell (Labclinics, S.A., Barcelona, Spain). 3-(4,5-dimethyl-2-thiazolyl)-2,5-diphenyl-2H-tetrazolium bromide (MTT) and Sodium polyphosphate (TPP) were obtained from VWR (Radnor, PA, USA).

2.2. Methods

2.2.1. Extraction of polysaccharides from macroalga Osmundea sp.

Before the extraction process, the dry macroalgal samples were subjected to a pre-treatment which consisted of the depigmentation and washing of the biomass by immersion the samples into a solution of acetone/ethanol and distilled water, respectively. Then, the freeze-drying and milling process was performed to obtain dried biomass with the highest surface-to-volume ratio during the latter extraction procedures.

After that, the dried algal samples were re-suspended in distilled water in the ratio of 1:60 (*w/v*), and the polysaccharides were extracted through 3 cycles of autoclave pressure (120 °C for 30 min). The extract was centrifuged at 3000 rpm^{-1} to remove residues, and the polysaccharides were precipitated with a triple volume of 96% ethanol. The precipitate was centrifuged at 3000 rpm^{-1}, dissolved in distilled water, and freeze-drying.

2.2.2. Characterisation of physicochemical properties of polysaccharides

The physicochemical properties of polysaccharides extracted from *Osmundea* sp. macroalgae samples were determined and compared the alginate and carrageenan.

To accomplish that, Fourier Transform Infrared Spectroscopy (FTIR) analysis was performed. The spectra were acquired by using an average of 128 scans, with a spectral width ranging from 400 cm^{-1} to 4000 cm^{-1} and a spectral resolution of 32 cm^{-1}. All the samples were placed on a diamond window, and the spectra were recorded using a Nicolet iS10 FTIR spectrophotometer (Thermo Scientific, Waltham, MA, USA).

In turn, the surface charge of the polysaccharides was characterised through Zetasizer Nano ZS equipment (Malvern Instruments, Worcestershire, UK), and the characteristic UV spectrum of polysaccharides was

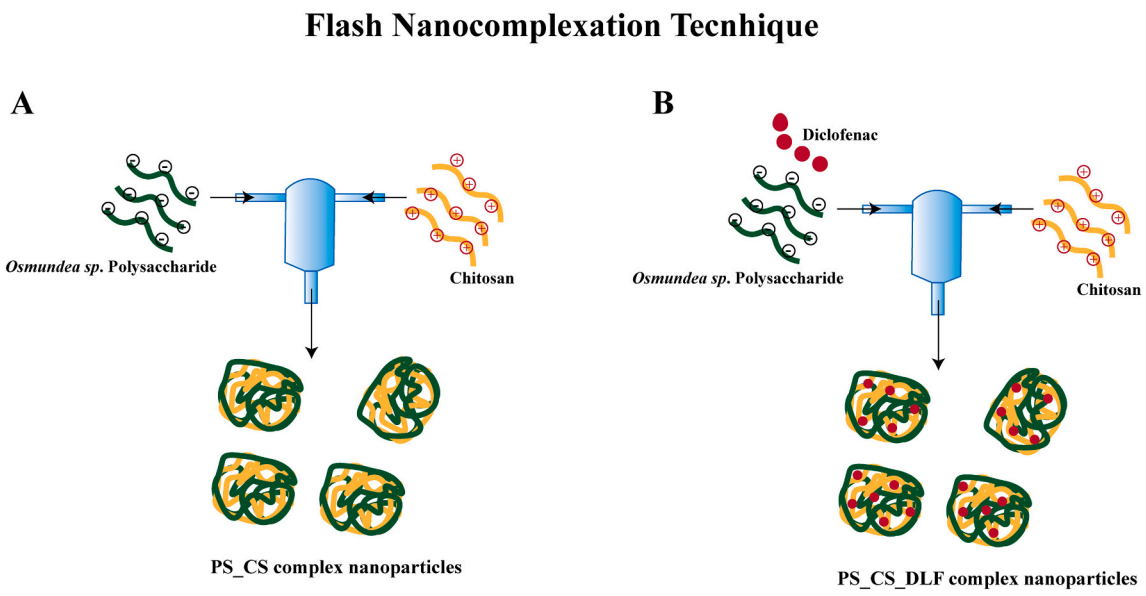

Fig. 1. Schematic representation of the flash nanocomplexation technique used in this work to produce the PS_CS (A) and PS_CS_DLF (B) nanoparticles.

also acquired by using the Thermo Scientific Multiskan GO UV/Vis spectrophotometer.

The determination of sulphate groups in polysaccharides samples was achieved by following the barium chloride-gelatin turbidity method already described in the literature [29,30].

In brief, the precipitation solution was prepared by mixing 0.3% gelatin solution, $BaCl_2$ and HCl. After that, about 0.20 mL of polysaccharide solution (1.0 mg/mL) was added to the precipitation solution, and the reaction occurred for 10–20 min. A blank was prepared with 0.2 mL of water instead of a precipitation solution. The released barium sulphate suspension was measured at $\lambda = 420$ nm by UV–VIS spectrophotometry using sodium sulphate as standard. The standard curve was registered with regression equation of: $Y = 0.0201 + 0.0402X$, $n = 5$, $R^2 = 0.99$. The sulphate ion is precipitated in a strongly acid medium with barium chloride through this method. The resulting turbidity is measured at 420 nm and compared with standard solutions.

2.2.3. Production of the polysaccharide-based nanoparticles loaded with Diclofenac

The production of the nanoparticles was accomplished through the flash nanocomplexation method (as illustrated in Fig. 1). In brief, the interaction between the negative surface charge of polysaccharides extracted from Osmundea sp. macroalgae and the positive charge of amine groups available on the chitosan backbone was promoted.

With the rapid and turbulent mixing between the PS and CS at a ratio of 1:4, it was possible to produce the nanoparticles (PS_CS). In addition, the diclofenac (DLF) (at a concentration of 1 mg/mL and 3 mg/mL) was incorporated into nanoparticles aims to obtain nanocarriers of anti-inflammatory drugs (PS_CS_DLF1 and PS_CS_DLF3). To accomplish that, the DLF was directly dissolved into a PS solution before the nanoprecipitation process. Nanoparticles without incorporated DLF were also produced for comparative purposes. In both types of nanoparticles, the TPP (1% *w/v*) solution was used as a collecting and stabilising solution of the nanosystems.

2.2.4. Characterisation of the morphological and physicochemical properties of nanoparticles

The morphology of nanoparticles was characterised by Transmission Electron Microscopy (TEM, Hitachi-HT7700, Japan) at an accelerating voltage of 80 kV.

In turn, the Zetasizer Nano ZS equipment (Malvern Instruments, Worcestershire, UK) was used the measure the nanoparticles' size and surface charge. Such parameters were determined at different time points to characterise the nanoparticles' stability when stored at room temperature and 4 °C.

The Fourier Transform Infrared (FTIR) spectra were also acquired on a Nicolet iS10 spectrometer, with a 4 cm^{-1} spectral resolution from 600 to 4000 nm (Thermo Scientific Inc., Massachusetts, USA) to confirm the presence of different compounds used in the nanoparticles' production.

2.3. Evaluation of the encapsulation efficiency of DLF into nanoparticles

The encapsulation and loading efficiency of DLF into nanoparticles was determined through the precipitation of the nanoparticles by using Amicon® Ultra-2 Centrifugal Filter Devices (30 k). Following the manufacturers' protocol, it was possible to recover the supernatant containing the free DLF. Then, the DLF was quantified through the Thermo Scientific Multiskan GO UV/Vis spectrophotometer and a standard absorbance curve ($y = 0.0117\ x + 3.5343$, $R^2 = 0.99$).

The UV absorbance spectra of nanoparticles without DLF was also recorded for control purposes. The encapsulation efficiency (EE) was determined using the following Eq. (1).

$$EE\ (\%) = \frac{W_i - W_s}{W_i} \times 100 \quad (1)$$

where W_i is the total amount of DLF added into PS_CS nanoparticles and W_s is the amount of DLF in the supernatant.

2.3.1. Characterisation of DLF release profile from nanoparticles

Afterwards, the amount of DLF released from nanoparticles solution was measured according to a method previously reported in the literature. The nanoparticles (at 1 mg/mL) were immersed in 5 mL of PBS at pH 8 or pH 5. Then, the samples were placed on a dialysis membrane (Spectrum™ Spectra/Por™ 6 8KD) and incubated at 37 °C under agitation to mimic the physiological conditions. At different time points, 1 mL of sample was recovered and replaced by the same volume. Afterwards, the supernatant absorbance was measured at 276 nm, using a Thermo Scientific Multiskan GO UV/Vis spectrophotometer to determine the amount of DLF released. All experiments were performed in triplicate.

Further, the drug-release kinetics exhibited by the produced membranes were also characterised by using the Peppas-Korsmeyer Eq. (2) and Hixon-Crowell models Eq. (3) [31]:

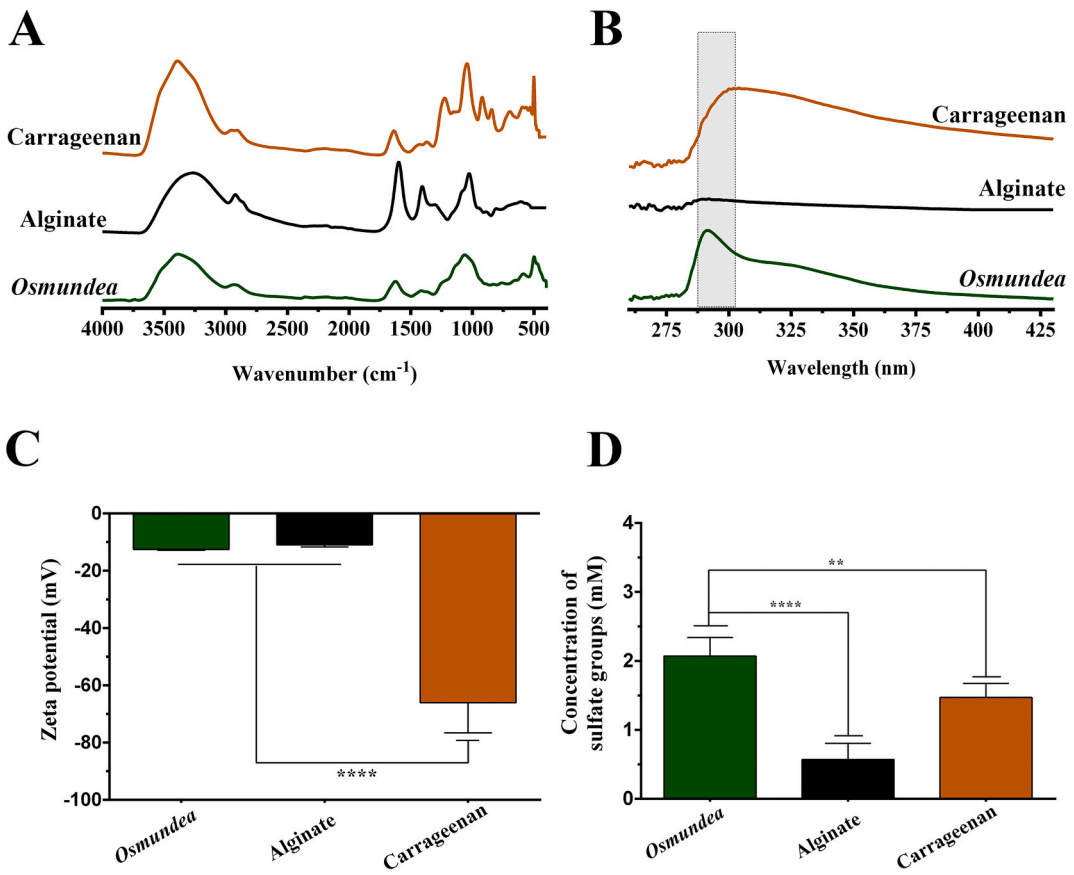

Fig. 2. Evaluation of the physiochemical properties of polysaccharide extracted from macroalgae *Osmundea* sp.: FTIR analysis (A), UV–visible spectroscopy (B), determination of zeta potential (C) and concentration of sulphate groups (D). Data are presented as mean ± standard deviation, $n = 3$, $^{**}p < 0.01$, $^{****}p < 0.0001$.

$$\text{Peppas} - \text{Korsmeyer} : \frac{M_t}{M_\infty} = \text{Kt}^n \quad (2)$$

$$\text{Higuchi} : Q_t = K_H\, t^{1/2} \quad (3)$$

where M_t is the cumulative amount of drug released at time t, M_∞ is the initial drug loading, K is a constant characteristic of the drug-polymer system, and n is the diffusion exponent, suggesting the nature of the release mechanism. Q_t is the amount of drug dissolved in time t, and K_H is the Higuchi dissolution constant.

2.3.2. Evaluation of cytotoxic profile of nanoparticles without/with Diclofenac in contact with fibroblasts and keratinocytes cells

The nanoparticles' biocompatibility was evaluated using an MTT assay recommended by the ISO 10993-5:2009 (Biological evaluation of medical devices- Part 5: Tests for in vitro cytotoxicity). The Normal Human Dermal Fibroblasts (NHDF) and human epidermal keratinocytes (HEK) cells were cultured in DMEM-F12, supplemented with 10% heat-inactivated FBS and amphotericin B (100 g/mL) in 75 cm^2 culture T-flasks. Then, the cells were seeded at a density of 5×10^3 cells per well and incubated at 37 °C, in an incubator with a 5% CO_2 humidified atmosphere.

After 24 h of incubation, the culture medium was replaced by the nanoparticles' solutions at different concentrations (from 2 mg/mL to 0.05 mg/mL). After 24, 48 and 72 h of incubation, the suspension of each well was removed and replaced by a mixture of 50 μL of MTT solution (5 mg/mL) and incubated for 4 h, at 37 °C, in a 5% CO_2 atmosphere. After that, the cells were treated with 100 μL of DMSO (0.04 N) for 30 min. The absorbance of each sample ($n = 5$) was determined at 570 nm using a microplate reader (Thermo Scientific Multiskan GO UV/Vis microplate spectrophotometer). Cells incubated with ethanol (96%) were used as a positive control (K^+), whereas cells incubated only with a culture medium were used as a negative control (K^-).

2.4. Statistical analysis

The statistical analysis of the obtained results was performed using one-way analysis of variance (ANOVA) with the Newman-Keuls post hoc test. A p-value lower than 0.05 ($p < 0.05$) was considered statistically significant.

3. Results and discussion

3.1. Characterisation of physicochemical properties of polysaccharide extracted from Osmundea sp.

Before the nanoparticles production, the PS was extracted from *Osmundea* sp. macroalgae, and their physicochemical properties were characterised (as presented in Fig. 2).

In general, spectroscopic methods, such as FTIR and UV–vis, are usually employed as a preliminary analysis of the molecular properties of a PS.

In this way, the FTIR spectrum of *Osmundea* sp.-PS (Fig. 2A) was acquired and compared with a sulphate (carrageenan) and non-sulphate polysaccharide (alginate) widely reported in the literature. Through the FITR spectra, it is possible to notice that PS displays peaks at 3389 cm^{-1} (-NH_2 and -OH groups), 2931 cm^{-1} (C—H asymmetric stretching). The peak at 1413 cm^{-1} resulted from the stretching vibration of C═O and the deformation vibration of OH (alcohols and phenols). In turn, the absorption peak at 1062 cm^{-1} (S═O stretch and glycosidic bonds) and 499 cm^{-1} (-C-O-SO_4 stretch) could be attributed to the presence of sulphate groups in the constitution of *Osmundea* sp.-PS [32–34].

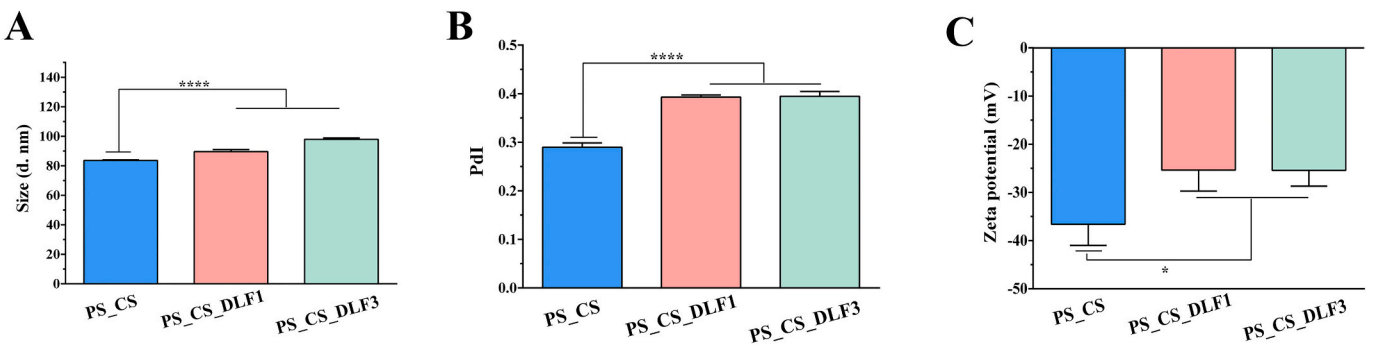

Fig. 3. Evaluation of morphological properties of unloaded CS_PS nanoparticles and loaded with DLF at concentration of 1 mg/mL and 3 mg/mL: determination of hydrodynamic diameter values of nanoparticles (A), index of polydispersity (B) and zeta potential (C). Data are presented as mean ± standard deviation, $n = 5$, * $< p = 0.05$, **** $p < 0.0001$.

On the other side, the peaks of alginate were visible at 3268 cm^{-1} (-OH stretch of water and -OH groups of the G and M units of alginate), 1600 cm^{-1} and 1406 cm^{-1} that correspond to the C═O stretching vibration of the carboxylic group of alginate [35,36]. In turn, the peaks of carrageenan appear at 3992 cm^{-1} (O—H stretch), 1042 cm^{-1} (O=S=O symmetric vibration) and 920 cm^{-1} (C_4-O-S stretching vibration) [37,38].

It is possible to verify that the *Osmundea* sp.-PS presented more similarities with the FTIR spectrum of carrageenan, indicating the presence of sulphate groups on their constitution.

In addition, UV–visible spectroscopy was also used to analyse the chromophore groups of atoms characterised by strongly absorbing electronic transitions [33]. The UV–visible absorption spectrum of the PS, alginate and carrageenan (Fig. 2B) indicated that the PS and carrageenan presented a higher UV area than the alginate. Specifically, the maximum absorption ranged from 260 to 280 nm, commonly attributed to the $\pi-\pi^*$ electron transitions in aromatic and poly-aromatic compounds found in most conjugated molecules, including proteins. These results indicate that *Osmundea* sp.-PS can be composed of different compounds (proteins, nucleic acids) that contain multiple UV-absorbing groups [33,39].

Furthermore, the DLS analysis was conducted to determine the surface charge of *Osmundea* sp.-PS, revealing that macroalgae PS possesses an anionic character with a zeta potential value of −12.57 ± 0.31 mV (as presented in Fig. 2C). Such value was similar to the alginate (−10.97 ± 0.74 mV), whereas the carrageenan showed a more negative charge (−66.10 ± 10.51 mV). Such anionic character of *Osmundea* sp.-PS enables to explore the possible electrostatic interactions with positively charged groups of other PS and bioactive compounds. Likewise, the anionic surface of PS is crucial to avoid aggregation during blood circulation.

Lastly, the concentration of sulphate groups of PS was determined through the barium chloride-gelatin turbidity method. This method induced the precipitation of sulphate ion, and the resulting turbidity was measured at 420 nm. The obtained results (Fig. 2D) are in agreement with the FTIR spectrum, revealing that the *Osmundea* sp. -PS and Carrageenan possessed sulphate groups on their composition.

3.2. Characterisation of morphological and physicochemical properties of nanoparticles

The study of the physicochemical properties of the *Osmundea* sp.- PS allowed their use in the production of polymeric nanoparticles (NPs) by flash nanocomplexation technique. Through this method, the electrostatic interaction between negatively charged groups of PS and positively charged groups of CS is promoted by a rapid mixing between compounds. Moreover, DLF at 1 mg/mL and 3 mg/mL was incorporated into NPs, aiming to develop a drug delivery system to treat inflammatory skin diseases. So, the unloaded nanoparticles were defined as CS_PS, whereas the nanoparticles incorporating 1 and 3 mg/mL of DLF were designed as CS_PS_DLF1 and CS_PS_DLF3, respectively.

Indeed, the flash nanocomplexation technique allowed the production of spherical nanoparticles through a rapid (2 s) and reproducible method. In turn, the DLS analysis revealed that these nanoparticles had a mean hydrodynamic diameter value of 83.54 ± 0.50 nm, 89.58 ± 1.42 nm and 97.92 ± 0.94 nm for PS_CS, PS_CS_DLF1 and PS_CS_DLF3 nanoparticles, respectively (as shown in Fig. 3 and size distribution by intensity showed in Fig. S1).

The increase in the hydrodynamic diameter size of the NPs with the drug incorporation was also noticed by other researchers. For example, Azizian S. et al. verified that the mean size of CS/TPP nanoparticles increased from 266 ± 5.33 nm to 415 ± 8.66 nm when BSA was incorporated [40].

Furthermore, the hydrodynamic diameter values lower than 100 nm are widely considered as suitable for dermal and transdermal drug delivery, and most of the studies evidenced that these nanoparticles enhanced the drug penetration into and across the skin, facilitating the drug activity and tolerability [24,25,41]. The skin permeability of nanoparticles is a crucial parameter in skin drug delivery applications. Such a feature has been recognised as an attractive property for nanoparticles since the small size of nanoparticles facilitates the permeation of the outer *stratum corneum* skin layer. Moreover, some authors also observed that nanoparticles could penetrate deeper into the skin layer, even reaching the systemic circulation [25]. On the other hand, chitosan was selected since it can act as a skin permeation enhancer by altering the keratin structure [42]. The hydrophilic hydroxyl groups of chitosan contribute to its hygroscopic properties, improve the water content in the stratum corneum, and increase cell membrane fluidity. In addition, the small size of the produced nanoparticles (below 100 nm) makes them suitable for diclofenac through the skin, which was already corroborated by different authors [43–46].

The penetration of nanoparticles through the skin may occur via lipid channels and/or the follicular route [47]. Due to the morphological properties of nanoparticles produced in this work, they would be penetrating the superficial layers of the *stratum corneum* and then releasing the encapsulated diclofenac into the deeper skin layers. The topical application of these nanocarriers would significantly increase the drug bioavailability in the epidermis, suggesting that this nanosystem may be used for transdermal delivery therapies for inflammatory skin disorders.

Another critical parameter to determine the success of NPs production is the polydispersity index which indicates the heterogeneity of the NPs population. The results showed that the produced NPs presented a low polydispersity with values lower than 0.5. Such values highlighted the reproductivity and efficiency of the flash nanocomplexation method to produce polymeric nanoparticles with a narrow size distribution as well as with the low tendency to aggregate [48].

Moreover, the zeta potential values revealed that all produced

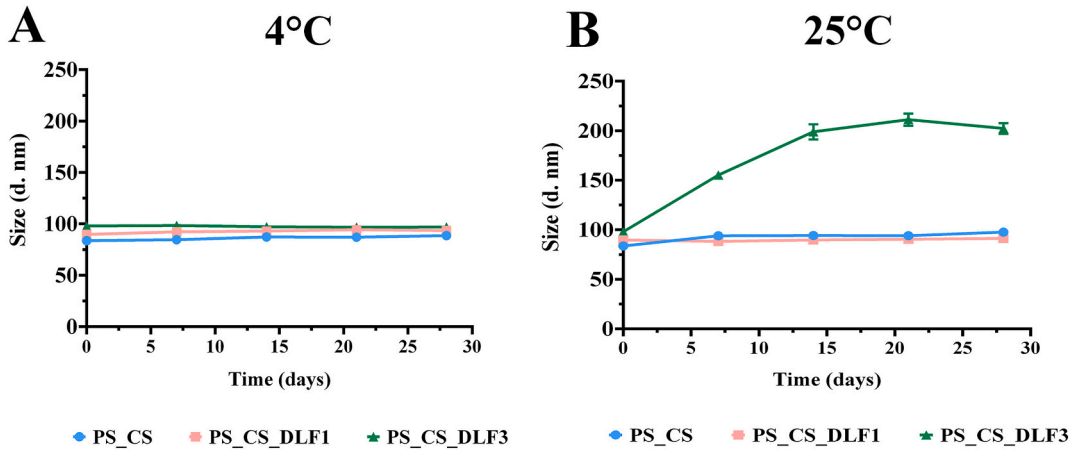

Fig. 4. Determination of nanoparticles' size after 7, 14, 21 and 28 days stored at 4 °C (A) and 25 °C (B).

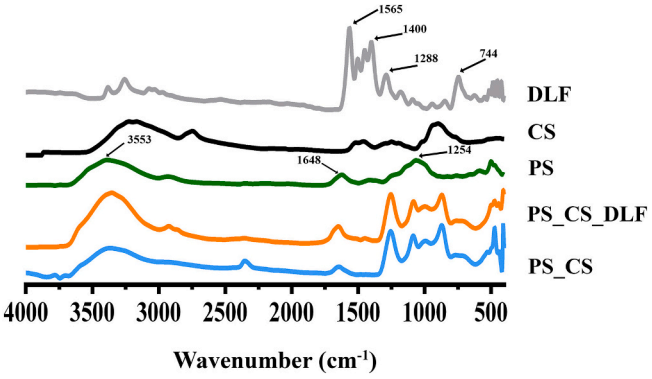

Fig. 5. ATR-FTIR analysis of the nanoparticles (PS_CS and PS_CS_DLF) and raw materials used for their synthesis (PS, CS and DLF).

nanoparticles possessed a negative surface charge with a zeta potential value of −36.6 ± 0.50 mV, −25.37 ± 4.36 mV and −25.43 ± 3.25 mV for PS_CS, PS_CS_DLF1 and CS_PS_DLF3 nanoparticles.

Such negative zeta potential indicated a prevalence of negatively charged groups, suggesting the presence of *Osmundea* sp. -PS on the particle surface.

For PS_CS_DLF1 and PS_CS_DLF3 nanoparticles, the zeta potential values decreased to ≈−25 mV, indicating that the addition of DLF interferes with the electrostatic interaction between *Osmundea* sp. -PS and CS, as verified in the hydrodynamic diameter size values.

The magnitude of the nanoparticles' zeta potential with values <−30 mV and >+30 mV is representative of stable NPs in suspension [49,50].

Further, the stability of nanoparticles was examined by monitoring changes over time when the NPs were stored in an aqueous solution at 4 °C and room temperature (25 °C) (as shown in Fig. 4). Along this incubation time, the results evidenced that the hydrodynamic diameter values remained stable when incubated at 4 °C. However, when the storage conditions used were at 25 °C, the PS_CS and PS_CS_DLF1 nanoparticles maintained their size, whereas the hydrodynamic diameter of PS_CS_DLF3 nanoparticles increased along with time incubation, indicating NPs aggregation.

Such results indicate that the produced NPs would be stable under storage and may have high stability in blood circulation after systemic administration. The stability of the NPs can be explained due to the strong electrostatic interactions between *Osmundea* sp.-PS and CS.

On the other hand, these findings are consistent with those obtained by He et al., who found that the NPs of CS/TPP also stable along 30 days at room temperature, not presenting significant alterations in NPs diameter (45 ± 1.4 nm to 47.6 ± 2.9 nm) [10].

Considering all morphological properties of NPs, the flash nanocomplexation technique demonstrated their excellent efficiency to produce *Osmundea* sp.-PS-based nanoparticles with suitable size and stability to be used in drug delivery and/or regenerative medicine applications.

Apart from the morphological properties, ATR-FTIR analysis was also done to characterise the synthesis of nanoparticles (Figure 5). In this way, the FTIR spectrum of nanoparticles as well as raw materials (CS, PS and DLF) were acquired.

The FTIR spectrum of CS exhibited as characteristic peaks: 3293 cm^{-1} (-OH stretch), 2871 cm^{-1} (aliphatic C—H stretch), 1648 cm^{-1} (NH_2 stretch), 1374 cm^{-1} (-C-O stretching of the primary alcohol group) and at 1026 cm^{-1} (C-O-C glycosidic bond), which are common to the *Osmundea* sp.-PS (as described in Section 3.1).

In turn, the FTIR spectrum of DLF showed the prominent peaks at 1564 cm^{-1} (C═O stretching), 1400 cm^{-1} (C═C stretching of carboxyl groups), 1288 cm^{-1} and 744 cm^{-1} that correspond to the C—N stretching [51].

In the FTIR spectrum of PS_CS and PS_CS_DLF nanoparticles, the different characteristic peaks of PS, CS and DLF appeared without significant shifting. In short, the electrostatic interaction between compounds and the flash nanocomplexation technique did not compromise the chemical integrity of PS and CS. Further, the DLF incorporation did not interact with the polysaccharides. So, the FTIR analysis confirmed the compatibility of the DLF with *Osmundea* sp.- PS and CS to prepare

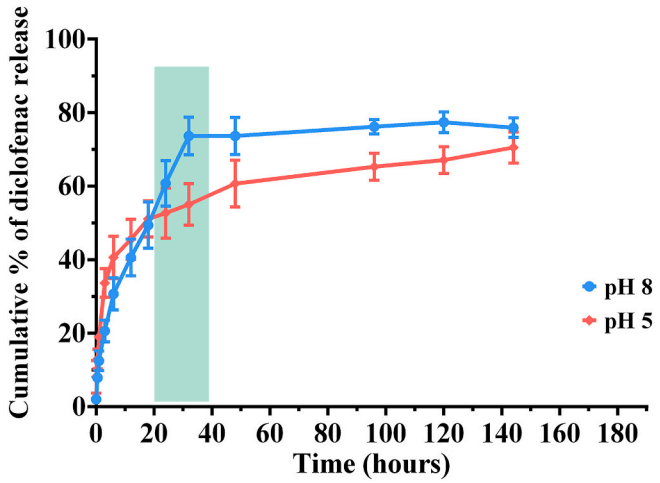

Fig. 6. Characterisation of the release profile of diclofenac from nanoparticles at pH 5(native skin) and pH 8 (injured skin).

Table 1
Regression coefficients of mathematical models fitted to the release of diclofenac from the PS_CS nanoparticles at pH 5 and pH 8.

		Hixon-Crowell	Korsmeyer-Peppas	
		R^2	R^2	n
pH 5	PS_CS_DLF	0.98	0.99	0.4
pH 8	PS_CS_DLF	0.99	0.99	0.5

nanoparticles.

3.3. Characterisation of diclofenac release profile from nanoparticles

Herein, DLF (an anti-inflammatory drug) was chosen to be loaded into the nanoparticles to be applied as a therapeutic approach to inflammatory skin diseases.

The encapsulation efficiency obtained for the DLF incorporation into the nanoparticles was 83.43 ± 0.82%, indicating that DLF can be encapsulated into nanosystems using the flash nanocomplexation technique. In turn, the drug loading was approximately about 1 mg of Diclofenac per 12 mg of nanoparticles. Afterwards, the in vitro release of DLF from PS_CS nanoparticles was investigated in a simulated physiological environment of healthy and injured skin (PBS, pH 5.5 and pH 8), following the indications described in the literature [52], where it is recommended the preparation of a fluid with a pH between 4.5 and 5.4 to evaluate the in vitro release of nonsteroidal anti-inflammatory drugs.

As shown in Fig. 6, the cumulative DLF release (100% of total drug released) profile exhibits an initial burst release (≈45% of DLF is released in the first 20 h of incubation), following a sustained release during at least 140 h. Such release profile can be related to the high surface to volume ratio of the nanoparticles that favour the PBS adsorption and hence the diffusion of DLF from the nanocarriers.

The cumulative release of DLF from the nanoparticles was 70.51 ± 4.23% and 85.90 ± 2.67% at pH 5 and pH 8, respectively. The protonation/deprotonation of CS can explain such differences at different pHs values. It is well described that the CS is deprotonated at pH > 7, making the nanoparticle more unstable and susceptible to disintegration, resulting in the release of DLF [10].

However, the release profile of DLF from nanoparticles is compatible with the inflammatory conditions (pH 8) and the peak of the inflammatory phase (1–3 days after skin injury).

Furthermore, the release data was also analysed by different mathematical kinetic models to characterise the type of interactions that influence the drug release (please see Table 1). The mathematical model that exhibits the best fitting with the obtained release data is the Korsmeyer-Peppas ($R^2 = 0.99$ ($n > 0.5$) at both pHs). Such indicates that the DLF is released from the PS_CS nanoparticles through a Fickian diffusion process that occurs due to the swelling of the polymeric matrix. Moreover, the first phase of the DLF release profile could also be fitted to the Higuchi model ($R^2 = 0.98$ at pH 5 and $R^2 = 0.99$ at pH 8), which attributes the initial burst release to the diffusion of DLF located on the nanoparticle surfaces [28,53].

Therefore, it can be concluded that the drug release from PS_CS nanoparticles occurs due to the diffusion of the DLF from nanoparticles' surface and dissolution of DLF from the polymeric matrix. The drug release kinetics models as mathematical approximation support the

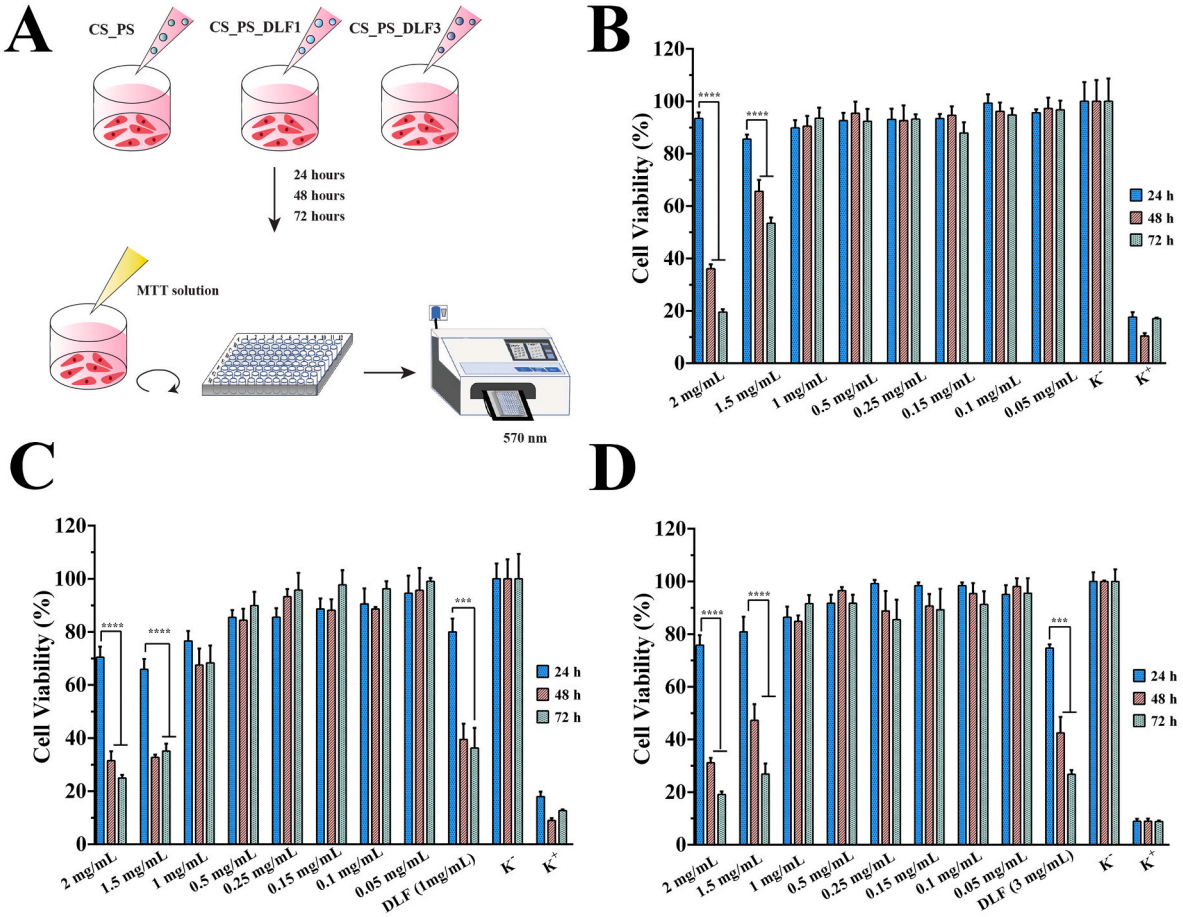

Fig. 7. Illustrative representation of the methodology involved in MTT assay (A) to characterise the cytotoxic profile of PS_CS (B), PS_CS_DLF1 (C) and PS_CS_DLF3 (D) nanoparticles at different concentrations (2 mg/mL- 0.05 mg/mL)) and the free diclofenac (DLF) drug at 1 mg/mL and 3 mg/mL in contact with human dermal fibroblast cells during 24 h, 48 h and 72 h. Data are presented as mean ± standard deviation, $n = 5$, ****$p < 0.0001$.

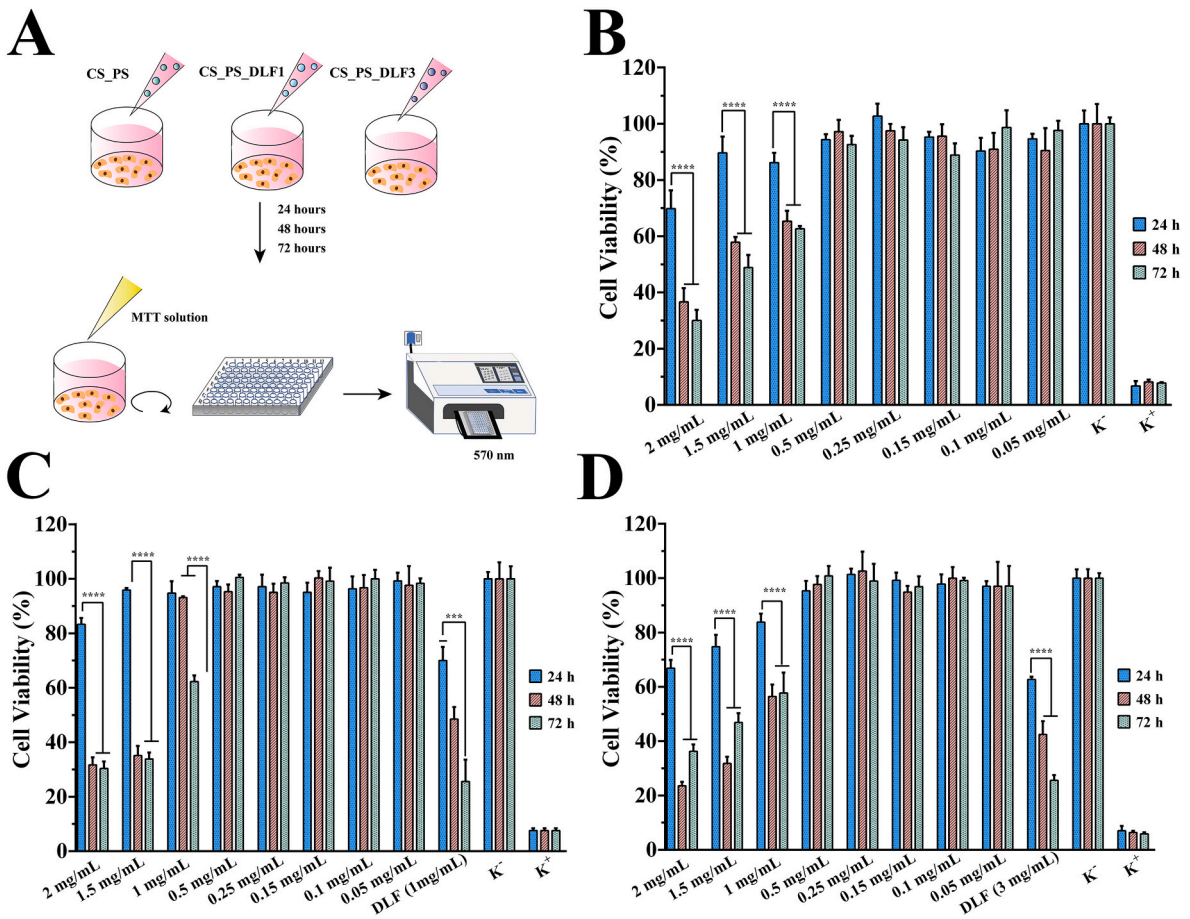

Fig. 8. Illustrative representation of the methodology involved in MTT assay (A) to characterise the cytotoxic profile of PS_CS (B), PS_CS_DLF1 (C) and PS_CS_DLF3 (D) nanoparticles at different concentrations (2 mg/mL- 0.05 mg/mL) and the free diclofenac (DLF) drug at 1 mg/mL and 3 mg/mL in contact with human epidermal keratinocytes cells during 24 h, 48 h and 72 h. Data are presented as mean ± standard deviation, n = 5, ****p < 0.0001.

mechanisms associated with nanoparticles' drug release. The drug release profile of diclofenac from dissolution/degradation of the nanoparticles was considered less probable since the size and surface charge of the nanoparticles was stable for at least 28 days.

In addition, the peak of DLF release after 24 h–48 h after incubation is coincident with the occurrence of the inflammation mechanisms (recruitment of neutrophils, monocyte/macrophages and lymphocytes decontaminate the wound, remove apoptotic neutrophils, and exert a specific response against microbes) [54].

3.4. Characterisation of biological properties of the nanoparticles

The cytocompatibility of the nanoparticles was evaluated by using NHDF and KEC as model cells. These cells are actively involved in different processes during the wound healing process, such as the production of ECM compounds and the maintenance of the protective epidermis layer. The NHDF are essential cells to tissue repair, one of the first cells to appear in injured sites. In turn, the KEC play a significant role in the immune skin response by releasing pro-inflammatory cytokines, chemokines, growth factors, proteases and matrix metalloproteinases [55–57].

So, the optical microscopic images of the NHDF and KEC cells seeded in contact with different concentrations of PS_CS, PS_CS_DLF1 and PS_CS_DLF3 nanoparticles after 24, 48 and 72 h (Figs. S2–S7) showed that cell morphology is compromised when the concentration of the nanoparticles is higher than 1 mg/mL after 48 h of incubation. However, for nanoparticles' concentration lower than 1 mg/mL, both types of cells exhibited similar morphology to those presented in the negative control (cells incubated only with culture medium).

In addition, the MTT assay performed over 24, 48, and 72 h corroborated the microscopic visualisations, i.e., the nanoparticles concentration lower than 1 mg/mL did not induce any cytotoxic effect on NHDF (Fig. 7) and KEC (Fig. 8) cells.

Nonetheless, it is relevant to perceive that the amount of DLF induced a more pronounced decrease in cell viability at high concentrations of nanoparticles (2 mg/mL and 1.5 mg/mL), which can be related to the intrinsic toxicity of the DLF [58,59].

On the other side, the KEC cells seem to be more susceptible to nanoparticles' action, presenting a significant decrease in cell viability at nanoparticles concentration of 1 mg/mL after 48 h of incubation. Such difference observed between NHDF and KEC cells could be related to the cell proliferation rate of KEC cells since they have a higher proliferative ability than NHDF cells and autocrine secretion of growth factors from the epidermal growth factor family, which are essential for the epidermal functions [60,61].

Also, the results showed the cytotoxicity of free diclofenac at concentrations (1 mg/mL and 3 mg/mL) on the fibroblasts and keratinocytes cells and at different time points of incubation. These results corroborated to the other works that have been verified the cytotoxicity of diclofenac, explaining the underlying mechanisms associated with this effect, where they appointed the diclofenac induced toxicity is justified by a decrease in ATP levels [62], cytochrome-mediated metabolism by microsomes, activation of caspase 3,8 and 9 [63], and oxidative stress for leucocytes [64].

Despite the toxicity associated with the free diclofenac, it should be noticed that its incorporation into polymeric nanodevice significantly

decreases the cytotoxic effect. Such fact highlights the promising potential of these nanocarriers in the treatment of inflammatory skin diseases because the drug incorporation will allow sustained and controlled delivery without compromising the skin cells viability and avoiding the administration times and consequently the cytotoxic effects.

Overall, the obtained results demonstrated the excellent biological performance of the unloaded and loaded PS_CS nanoparticles at concentrations lower than 1 mg/mL which can be used as a drug delivery system to treat inflammatory skin disorders.

4. Conclusions

In general, the macroalgae polysaccharides presented importance and relevance for pharmaceutical biotechnology applications due to i) the presence of glycosidic bonds that can be easily cleaved by hydrolase enzymes; and ii) the presence of the negatively charged sulphate groups that potentiate the polyelectrolyte behaviour and functionalisation. In this way, techniques such as ionotropic gelation and bulk mixing have been widely used to produce macroalgae polysaccharides-based nanoparticles. However, these methodologies did not assure the reproducibility and stability of nanoparticles.

Thus, in this work, the polysaccharide extracted from *Osmundea* sp. was used to produce nanoparticles by using the flash nanocomplexation technique, combining the negatively charged groups of the PS with the positively charged groups of CS. Also, DLF was incorporated into nanosystems to obtain a drug delivery system adequate for treating inflammatory skin disorders.

Overall, the results suggested that the nanoparticles presented hydrodynamic diameter values (< 100 nm) and stability compatible with skin delivery. Further, the DLF was released from nanoparticles in a sustained manner, which is crucial to avoid an exuberant and prolonged inflammation response. More yet, the nanoparticles did not induce any cytotoxic effect on fibroblast and keratinocytes cells at concentrations lower than 1 mg/mL, emphasising their suitability to be used as a therapeutic approach.

Also, these nanoparticles could be incorporated into 3D systems (membranes, sponges, hydrogels) aims to facilitate the wound healing process and/or can be loaded with other drugs (e.g. antibiotics, antiviral, anticancer drugs, etc.), spreading the application of these nanosystems for other biomedical fields. In the future, ex vivo and in vivo assays can be performed further to evaluate the potential of the nanoparticles for skin regeneration and accelerate the clinical translation.

CRediT authorship contribution statement

Sónia P. Miguel: Conceptualization, Methodology, Investigation, Validation, Writing- Reviewing and Editing; Jorge Loureiro: Methodology, Investigation, Writing- Reviewing and Editing; Maximiano P. Ribeiro: Investigation, Formal analysis, Writing- Reviewing and Editing; Paula Coutinho: Conceptualization, Methodology, Investigation, Validation, Project administration, Writing- Reviewing and Editing.

Acknowledgments

This work was financed by the 0558_ALGALUP_6_E “Integral alternative for the exploitation of macroalgae in the area of Galicia and Portugal”, which was co-financed by the European Regional Development Fund (ERDF) through the Program INTERREG V-A Spain-Portugal (POCTEP) 2018-2021. Jorge Loureiro acknowledges BioimpACE project for the funding given on the form of fellowship.

Appendix A. Supplementary data

Supplementary data to this article can be found online at https://doi.org/10.1016/j.ijbiomac.2022.01.180.

References

[1] J. Venkatesan, S. Anil, S.-K. Kim, M.S. Shim, Seaweed polysaccharide-based nanoparticles: preparation and applications for drug delivery, Polymers 8 (2) (2016) 30.
[2] T.H. Silva, A. Alves, E.G. Popa, L.L. Reys, M.E. Gomes, R.A. Sousa, S.S. Silva, J. F. Mano, R.L. Reis, Marine algae sulfated polysaccharides for tissue engineering and drug delivery approaches, Biomatter 2 (4) (2012) 278–289.
[3] S. Ermakova, M. Kusaykin, A. Trincone, Z. Tatiana, Are multifunctional marine polysaccharides a myth or reality? Front. Chem. 3 (2015) 39.
[4] Y. Luo, Food colloids binary and ternary nanocomplexes: innovations and discoveries, Colloids Surf. B: Biointerfaces 196 (2020), 111309.
[5] Y. Luo, Q. Wang, Y. Zhang, Biopolymer-based nanotechnology approaches to deliver bioactive compounds for food applications: a perspective on the past, present, and future, J. Agric. Food Chem. 68 (46) (2020) 12993–13000.
[6] H.-W. Sung, K. Sonaje, Z.-X. Liao, L.-W. Hsu, E.-Y. Chuang, pH-responsive nanoparticles shelled with chitosan for oral delivery of insulin: from mechanism to therapeutic applications, Acc. Chem. Res. 45 (4) (2012) 619–629.
[7] Y.-H. Lin, K. Sonaje, K.M. Lin, J.-H. Juang, F.-L. Mi, H.-W. Yang, H.-W. Sung, Multi-ion-crosslinked nanoparticles with pH-responsive characteristics for oral delivery of protein drugs, J. Control. Release 132 (2) (2008) 141–149.
[8] A. Fàbregas, M. Miñarro, E. García-Montoya, P. Pérez-Lozano, C. Carrillo, R. Sarrate, N. Sánchez, J. Ticó, J. Suñé-Negre, Impact of physical parameters on particle size and reaction yield when using the ionic gelation method to obtain cationic polymeric chitosan–tripolyphosphate nanoparticles, Int. J. Pharm. 446 (1–2) (2013) 199–204.
[9] A. Elsayed, M. Al-Remawi, N. Qinna, A. Farouk, K.A. Al-Sou'od, A.A. Badwan, Chitosan–sodium lauryl sulfate nanoparticles as a carrier system for the in vivo delivery of oral insulin, Aaps Pharmscitech 12 (3) (2011) 958.
[10] Z. He, J.L. Santos, H. Tian, H. Huang, Y. Hu, L. Liu, K.W. Leong, Y. Chen, H.-Q. Mao, Scalable fabrication of size-controlled chitosan nanoparticles for oral delivery of insulin, Biomaterials 130 (2017) 28–41.
[11] S. Cook, Flash Nano-complexation: A Tunable Technique for Electrostatically Driven Nanoparticle Fabrication, 2018.
[12] Y. De Anda-Flores, A. Rascón-Chu, A.C. Campa-Mada, J. Lizardi-Mendoza, J. Tanori-Cordova, E. Carvajal-Millan, systems, in: Natural Polysaccharides in Drug Delivery and Biomedical Applications, Elsevier, 2019, pp. 399–417.
[13] X. Ke, H. Tang, H.-Q. Mao, Effective encapsulation of curcumin in nanoparticles enabled by hydrogen bonding using flash nanocomplexation, Int. J. Pharm. 564 (2019) 273–280.
[14] D. Rodrigues, A.C. Freitas, L. Pereira, T.A. Rocha-Santos, M.W. Vasconcelos, M. Roriz, L.M. Rodríguez-Alcalá, A.M. Gomes, A.C. Duarte, Chemical composition of red, brown and green macroalgae from buarcos bay in central west coast of Portugal, Food Chem. 183 (2015) 197–207.
[15] D. Rodrigues, A.R. Costa-Pinto, S. Sousa, M.W. Vasconcelos, M.M. Pintado, L. Pereira, T.A. Rocha-Santos, J.P.D. Costa, A. Silva, A.C. Duarte, Sargassum muticum and Osmundea pinnatifida enzymatic extracts: chemical, structural, and cytotoxic characterisation, Mar. Drugs 17 (4) (2019) 209.
[16] S. Patel, Therapeutic importance of sulfated polysaccharides from seaweeds: updating the recent findings, 3Biotech 2 (3) (2012) 171–185.
[17] E. Percival, The polysaccharides of green, red and brown seaweeds: their basic structure, biosynthesis and function, Br. Phycol. J. 14 (2) (1979) 103–117.
[18] F.B. Pimentel, R.C. Alves, F. Rodrigues, M.B.P.P. Oliveira, Macroalgae-derived ingredients for cosmetic industry—an update, Cosmetics 5 (1) (2018) 2.
[19] A. Leandro, L. Pereira, A.M. Gonçalves, Diverse applications of marine macroalgae, Mar. Drugs 18 (1) (2020) 17.
[20] Y.C. Huang, U.I. Lam, Chitosan/fucoidan pH sensitive nanoparticles for oral delivery system, J. Chin. Chem. Soc. 58 (6) (2011) 779–785.
[21] A. Grenha, M.E. Gomes, M. Rodrigues, V.E. Santo, J.F. Mano, N.M. Neves, R. L. Reis, Development of new chitosan/carrageenan nanoparticles for drug delivery applications, J. Biomed. Mater. Res. A 92 (4) (2010) 1265–1272.
[22] H. Thai, C.T. Nguyen, L.T. Thach, M.T. Tran, H.D. Mai, T.T.T. Nguyen, G.D. Le, M. Van Can, L. Dai Tran, G.L. Bach, Characterisation of chitosan/alginate/lovastatin nanoparticles and investigation of their toxic effects in vitro and in vivo, Sci. Rep. 10 (1) (2020) 1–15.
[23] M. SS , G. SG , Recent Nanotechnological Aspects In Cosmetics and Dermatological Preparations.
[24] I. Aranaz, N. Acosta, C. Civera, B. Elorza, J. Mingo, C. Castro, M.D.L.L. Gandía, A. Heras Caballero, Cosmetics and cosmeceutical applications of chitin, chitosan and their derivatives, Polymers 10 (2) (2018) 213.
[25] Q. Ta, J. Ting, S. Harwood, N. Browning, A. Simm, K. Ross, I. Olier, R. Al-Kassas, Chitosan nanoparticles for enhancing drugs and cosmetic components penetration through the skin, Eur. J. Pharm. Sci. 160 (2021), 105765.
[26] J.H. Hamman, Chitosan based polyelectrolyte complexes as potential carrier materials in drug delivery systems, Mar. Drugs 8 (4) (2010) 1305–1322.
[27] S.P. Miguel, M.P. Ribeiro, H. Brancal, P. Coutinho, I.J. Correia, Thermoresponsive chitosan–agarose hydrogel for skin regeneration, Carbohydr. Polym. 111 (2014) 366–373.
[28] P.I. Morgado, S.P. Miguel, I.J. Correia, A. Aguiar-Ricardo, Ibuprofen loaded PVA/chitosan membranes: a highly efficient strategy towards an improved skin wound healing, Carbohydr. Polym. 159 (2017) 136–145.
[29] K. Dodgson, R. Price, A note on the determination of the ester sulphate content of sulphated polysaccharides, Biochem. J. 84 (1) (1962) 106–110.
[30] P. Bhadja, C.-Y. Tan, J.-M. Ouyang, K. Yu, Repair effect of seaweed polysaccharides with different contents of sulfate group and molecular weights on damaged HK-2 cells, Polymers 8 (5) (2016) 188.

[31] Y. Fu, W.J. Kao, Drug release kinetics and transport mechanisms of non-degradable and degradable polymeric delivery systems, Expert Opin. Drug Deliv. 7 (4) (2010) 429–444.
[32] P. Seedevi, S. Sudharsan, S.V. Kumar, A. Srinivasan, S. Vairamani, A. Shanmugan, Isolation and characterisation of sulphated polysaccharides from Codium tomentosum (J. Stackhouse, 1797) collected from southeast coast of India, Adv. Appl. Sci. Res. 4 (5) (2013) 72–77.
[33] L. Trabelsi, N.H. M'sakni, H.B. Ouada, H. Bacha, S. Roudesli, Partial characterisation of extracellular polysaccharides produced by cyanobacterium Arthrospira platensis, Biotechnol. Bioprocess Eng. 14 (1) (2009) 27–31.
[34] H. El-Rafie, M. El-Rafie, M. Zahran, Green synthesis of silver nanoparticles using polysaccharides extracted from marine macro algae, Carbohydr. Polym. 96 (2) (2013) 403–410.
[35] J.C. Boga, S.P. Miguel, D. de Melo-Diogo, A.G. Mendonça, R.O. Louro, I.J. Correia, In vitro characterisation of 3D printed scaffolds aimed at bone tissue regeneration, Colloids Surf. B: Biointerfaces 165 (2018) 207–218.
[36] S.P. Miguel, C.S. Cabral, A.F. Moreira, I.J. Correia, Production and characterisation of a novel asymmetric 3D printed construct aimed for skin tissue regeneration, Colloids Surf. B: Biointerfaces 181 (2019) 994–1003.
[37] S. Abdullah, N.H. Azeman, N.N. Mobarak, M.S.D. Zan, A.A.A. Bakar, Sensitivity enhancement of localised SPR sensor towards Pb (II) ion detection using natural bio-polymer based carrageenan, Optik 168 (2018) 784–793.
[38] L. Fan, L. Wang, S. Gao, P. Wu, M. Li, W. Xie, S. Liu, W. Wang, Synthesis, characterisation and properties of carboxymethyl kappa carrageenan, Carbohydr. Polym. 86 (3) (2011) 1167–1174.
[39] R. Guo, X. Li, X. Chen, Y. Kou, H. Hu, X. Liu, D. Li, Y. Liu, L. Ai, Z. Song, An ultrasonic-extracted arabinoglucan from Tamarindus indica L. pulp: a study on molecular and structural characterisations, Int. J. Biol. Macromol. 164 (2020) 3687–3697.
[40] S. Azizian, A. Hadjizadeh, H. Niknejad, Chitosan-gelatin porous scaffold incorporated with chitosan nanoparticles for growth factor delivery in tissue engineering, Carbohydr. Polym. 202 (2018) 315–322.
[41] C.A. Ibekwe, G.M. Oyatogun, T.A. Esan, K.M. Oluwasegun, Synthesis and characterisation of chitosan/gum arabic nanoparticles for bone regeneration, Am. J. Mater. Sci. Eng. 5 (1) (2017) 28–36.
[42] C. Qin, Y. Du, L. Xiao, Y. Liu, H. Yu, Moisture retention and antibacterial activity of modified chitosan by hydrogen peroxide, J. Appl. Polym. Sci. 86 (7) (2002) 1724–1730.
[43] T. Caon, L.C. Porto, A. Granada, M.P. Tagliari, M.A.S. Silva, C.M.O. Simões, R. Borsali, V. Soldi, Chitosan-decorated polystyrene-b-poly (acrylic acid) polymersomes as novel carriers for topical delivery of finasteride, Eur. J. Pharm. Sci. 52 (2014) 165–172.
[44] Z. Zhang, P.C. Tsai, T. Ramezanli, B.B. Michniak-Kohn, Polymeric nanoparticles-based topical delivery systems for the treatment of dermatological diseases, Wiley Interdiscip. Rev. Nanomed. Nanobiotechnol. 5 (3) (2013) 205–218.
[45] B.N. Matos, T.A. Reis, T. Gratieri, G.M. Gelfuso, Chitosan nanoparticles for targeting and sustaining minoxidil sulphate delivery to hair follicles, Int. J. Biol. Macromol. 75 (2015) 225–229.
[46] A. Raber, A. Mittal, J. Schäfer, U. Bakowsky, J. Reichrath, T. Vogt, U. Schaefer, S. Hansen, C.-M. Lehr, Quantification of nanoparticle uptake into hair follicles in pig ear and human forearm, J. Control. Release 179 (2014) 25–32.
[47] M. Pelegrino, R. Weller, X. Chen, J. Bernardes, A.B. Seabra, Chitosan nanoparticles for nitric oxide delivery in human skin, MedChemComm 8 (4) (2017) 713–719.
[48] A.Y. Waddad, S. Abbad, F. Yu, W.L. Munyendo, J. Wang, H. Lv, J. Zhou, Formulation, characterisation and pharmacokinetics of morin hydrate niosomes prepared from various non-ionic surfactants, Int. J. Pharm. 456 (2) (2013) 446–458.
[49] S. Benita, M. Levy, Submicron emulsions as colloidal drug carriers for intravenous administration: comprehensive physicochemical characterisation, J. Pharm. Sci. 82 (11) (1993) 1069–1079.
[50] C.B. Woitiski, F. Veiga, A. Ribeiro, R. Neufeld, Design for optimisation of nanoparticles integrating biomaterials for orally dosed insulin, Eur. J. Pharm. Biopharm. 73 (1) (2009) 25–33.
[51] A.K. Nayak, D. Pal, Development of pH-sensitive tamarind seed polysaccharide–alginate composite beads for controlled diclofenac sodium delivery using response surface methodology, Int. J. Biol. Macromol. 49 (4) (2011) 784–793.
[52] M.R. Marques, R. Loebenberg, M. Almukainzi, Simulated biological fluids with possible application in dissolution testing, Dissolut. Technol. 18 (3) (2011) 15–28.
[53] S.U. Kumar, I. Matai, P. Dubey, B. Bhushan, A. Sachdev, P. Gopinath, Differentially cross-linkable core–shell nanofibers for tunable delivery of anticancer drugs: synthesis, characterisation and their anticancer efficacy, RSC Adv. 4 (72) (2014) 38263–38272.
[54] D. Simões, S.P. Miguel, M.P. Ribeiro, P. Coutinho, A.G. Mendonça, I.J. Correia, Recent advances on antimicrobial wound dressing: a review, Eur. J. Pharm. Biopharm. 127 (2018) 130–141.
[55] F.O. Nestle, P. Di Meglio, J.-Z. Qin, B.J. Nickoloff, Skin immune sentinels in health and disease, Nat. Rev. Immunol. 9 (10) (2009) 679–691.
[56] R. Di Caprio, S. Lembo, L. Di Costanzo, A. Balato, G. Monfrecola, Anti-inflammatory properties of low and high doxycycline doses: an in vitro study, Mediat. Inflamm. 2015 (2015).
[57] S.P. Miguel, M.P. Ribeiro, P. Coutinho, I.J. Correia, Electrospun polycaprolactone/aloe vera_chitosan nanofibrous asymmetric membranes aimed for wound healing applications, Polymers 9 (5) (2017) 183.
[58] S. Gomaa, Adverse effects induced by diclofenac, ibuprofen, and paracetamol toxicity on immunological and biochemical parameters in Swiss albino mice, J. Basic Appl. Zool. 79 (1) (2018) 5.
[59] L.J. Hunter, D.M. Wood, P.I. Dargan, The patterns of toxicity and management of acute nonsteroidal anti-inflammatory drug (NSAID) overdose, Open Access Emerg. Med. 3 (2011) 39.
[60] M.F. Denning, Epidermal keratinocytes: regulation of multiple cell phenotypes by multiple protein kinase C isoforms, Int. J. Biochem. Cell Biol. 36 (7) (2004) 1141–1146.
[61] L.E.N. Ferreira, B.V. Muniz, J. Burga-Sánchez, M.C. Volpato, E. de Paula, E.A. R. Rosa, F.C. Groppo, The effect of two drug delivery systems in ropivacaine cytotoxicity and cytokine release by human keratinocytes and fibroblasts, J. Pharm. Pharmacol. 69 (2) (2017) 161–171.
[62] R. Bort, X. Ponsoda, R. Jover, M.J. Gómez-Lechón, J.V. Castell, Diclofenac toxicity to hepatocytes: a role for drug metabolism in cell toxicity, J. Pharmacol. Exp. Ther. 288 (1) (1999) 65–72.
[63] M.J. Gómez-Lechón, X. Ponsoda, E. O'Connor, T. Donato, R. Jover, J.V. Castell, Diclofenac induces apoptosis in hepatocytes, Toxicol. in Vitro 17 (5–6) (2003) 675–680.
[64] M. Nemcova, J. Pikula, J. Zukal, V. Seidlova, Diclofenac-induced cytotoxicity in cultured carp leukocytes, Physiol. Res. 69 (2020).